

Review

Effect of H₂ on Blast Furnace Ironmaking: A Review

Chenchen Lan ^{1,*}, Yuejun Hao ², Jiannan Shao ¹, Shuhui Zhang ¹, Ran Liu ¹ and Qing Lyu ¹¹ College of Metallurgy & Energy, North China University of Science and Technology, Tangshan 063210, China² Caofeidian College of Technology, Tangshan 063210, China

* Correspondence: 15081586028@163.com

Abstract: Under the background of “carbon peaking” and “carbon neutralization”, the green transformation of iron and steel enterprises is imminent. The hydrogen-rich smelting technology of blast furnaces is very important for reducing energy consumption and CO₂ emission in ironmaking systems, and it is one of the important directions of green and low-carbon development of iron and steel enterprises. In this paper, the research status of the thermal state, reduction mechanism of iron-bearing burden, coke degradation behavior, and formation of the cohesive zone in various areas of blast furnace after hydrogen-rich smelting is summarized, which can make a more clear and comprehensive understanding for the effect of H₂ on blast furnace ironmaking. Meanwhile, based on the current research situation, it is proposed that the following aspects should be further studied in the hydrogen-rich smelting of blast furnaces: (1) the utilization rate of hydrogen and degree of substitution for direct reduction, (2) combustion behavior of fuel in raceway, (3) control of gas flow distribution in the blast furnace, (4) operation optimization of the blast furnace.

Keywords: blast furnace; H₂; heat consumption; reduction mechanism; cohesive zone; blast furnace operation



Citation: Lan, C.; Hao, Y.; Shao, J.; Zhang, S.; Liu, R.; Lyu, Q. Effect of H₂ on Blast Furnace Ironmaking: A Review. *Metals* **2022**, *12*, 1864. <https://doi.org/10.3390/met12111864>

Academic Editor: Pasquale Cavaliere

Received: 31 August 2022

Accepted: 28 October 2022

Published: 1 November 2022

Publisher's Note: MDPI stays neutral with regard to jurisdictional claims in published maps and institutional affiliations.



Copyright: © 2022 by the authors. Licensee MDPI, Basel, Switzerland. This article is an open access article distributed under the terms and conditions of the Creative Commons Attribution (CC BY) license (<https://creativecommons.org/licenses/by/4.0/>).

1. Introduction

On the background of “carbon peaking” and “carbon neutralization”, the transformation of traditional iron and steel metallurgical technology centered on “decarbonization” has become a new trend of green development of the iron and steel industry. Changing the energy consumption structure, replacing carbon with hydrogen, and realizing “low carbon” or even “zero carbon” is one of the directions to solve the environmental pollution and carbon emissions of the iron and steel industry.

In the process of blast furnace (BF) smelting, about 30% of iron oxides are reduced by CO, about 10% by H₂, and the rest by carbon [1]. The purpose of hydrogen-rich smelting in BF is to increase the proportion of H₂ reduction so as to reduce the consumption of carbon reductant. At present, domestic and foreign iron and steel enterprises attach great importance to the research of hydrogen energy ironmaking. One of the objectives of the Japanese Course50 (environmentally harmonious ironmaking) project is to replace some reductants in the BF with hydrogen and reduce the CO₂ emissions of the BF by 30% [2]. China Baowu Steel has carried out an industrial experiment of hydrogen-rich carbon circulating oxygen BF, achieving the reduction of 45 kg/tHM fuel ratio and 30% CO₂ reduction [3]. ThyssenKrupp Steel of Germany also officially launched the hydrogen ironmaking experiment, the BF uses part of hydrogen instead of coal for smelting, thus reducing the CO₂ emission by 20% [4]. The hydrogen metallurgy center of China Iron & Steel Research Institute Group has completed the R&D and industrial application of hydrogen injection into the tuyeres of two 1860 m³ BFs, the average fuel ratio of the BF has been reduced by 32 kg/tHM, and good economic, social, environmental, and carbon reduction effects have been achieved [5]. The Bremen plant of ArcelorMittal in Germany is preparing hydrogen through the electrolytic cell and injecting it into the BF, which can achieve the goal of reducing carbon consumption and CO₂ emissions in the BF

ironmaking process [6]. In addition, ArcelorMittal's Asturias Plant has started to inject hydrogen extracted from natural gas and coke oven gas into the BF in 2021 [6]. Dillinger and Saarstahl Steel in Germany jointly developed the coke oven gas injection process for BF and planned to inject pure hydrogen into two BFs, with the goal of reducing CO₂ emissions by 40% by 2035 [4,7]. At the same time, SSAB AB, POSCO, HBIS group, Jinghua Risteel, Jianlong group, Jiuquan Iron and Steel Co., Ltd., Anshan Iron and Steel Co., Ltd., Baotou Iron and Steel Co., Ltd. and Shanxi Zhongjin Steel Co., Ltd. also carried out the strategic layout of hydrogen energy [3,8]. The above facts show that scholars and technicians have fully realized the necessity and application value of developing hydrogen-rich smelting technology. According to statistics, the output of BF pig iron in China in 2021 is about 869 million tons, accounting for an absolute proportion of the structure of China's iron and steel industry [9]. China's ironmaking production process based on BF still occupies a dominant position for a long time in the future. Therefore, the development of hydrogen-rich smelting technology in BF is very important for reducing energy consumption and CO₂ emission of ironmaking systems in China.

Due to the increase of H₂ volume fraction in the BF, the thermal state, reduction mechanism of iron-bearing burden, coke degradation behavior, and formation of a cohesive zone in various areas of the BF have been greatly changed. At present, researchers have also made some research on the changes in these aspects. This paper summarizes the above aspects, summarizes the research results, and puts forward some problems and research directions in the hydrogen-rich smelting of BF, so as to help people understand the hydrogen-rich smelting of BF more clearly and comprehensively.

2. Effect of Hydrogen-Rich Smelting on Heat of Blast Furnace

2.1. Tuyere Raceway

After H₂ enters the BF from the tuyere, there is O₂ in the tuyere area, H₂ and O₂ will undergo a combustion reaction and release heat. However, the generated H₂O rapidly reacts with the carbon completely in the tuyere area to generate H₂ again and absorb heat. Therefore, it can be simply considered that H₂ only has a temperature rise process in the tuyere area, which consumes heat [10]. The heat calculation can be obtained from Equation (1).

$$\Delta H = \int_{25}^t V \times C_p \times dt \quad (1)$$

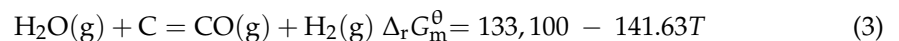
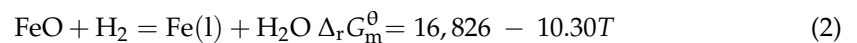
where: ΔH is heat absorption, kJ/t; t is the maximum temperature of H₂, K; V is the volume of H₂, m³/t; C_p is the constant pressure specific heat capacity of H₂, kJ/(m³·K); d is a differential sign.

At present, the main hydrogen production routes are coal to hydrogen, natural gas to hydrogen, methanol to hydrogen, and electrolytic water to hydrogen [11]. When hydrogen-rich gases from different sources are injected into the BF, the hydrogen-rich gas needs to consume part of the heat in the tuyere area of the BF during the heating process. When the hydrogen-rich gas contains hydrocarbons, they are converted into H₂ and CO through cracking under high-temperature conditions. The cracking process of the hydrocarbons and the increase of the gas volume after cracking all reduce the temperature in the tuyere area. Zhang et al. [12] pointed out that the natural gas injection volume increases from 20 m³/t to 25 m³/t, and the theoretical combustion temperature decreases from 2408.75 K to 2384.25 K, that is, the theoretical combustion temperature decreases by about 5 K for every 1 m³/tHM increase in the natural gas injection volume. Through industrial experiments and research, Gao et al. [5] found that the injection of hydrogen-rich gas into the tuyere reduced the theoretical combustion temperature. When 1 m³/tHM hydrogen-rich gas is injected, the theoretical combustion temperature of the tuyere is reduced by about 1.5 °C, and the blast volume and the gas volume in the bosh of the BF are reduced slightly. When hydrogen-rich gas is injected into the BF, the technology of high blast temperature and oxygen-enriched blast is usually adopted. By increasing the oxygen enrichment rate and

reducing the volume fraction of N_2 , the amount of gas in the hearth can be reduced and the reasonable theoretical combustion temperature of tuyere can be maintained [13–17].

2.2. Dripping Zone and Cohesive Zone

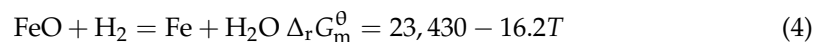
When high-temperature H_2 passes through the dripping zone and cohesive zone from the tuyere area, high-temperature H_2 further reduces the molten FeO or semi-molten FeO (Equation (2)), and H_2O is generated in the reduction process, which is an endothermic reaction. The steam continues to cause a gasification reaction with the coke and again converts to H_2 (Equation (3)). Due to the high temperature of the dripping zone and cohesive zone, almost all the generated steam can react with the coke. Therefore, the FeO in this region is still the direct reduction of coke in essence, but the presence of H_2 can accelerate the reaction. The research shows that [18,19], after the hydrogen-rich smelting of BF, due to the enhancement of the reduction ability of gas, the iron oxide is largely reduced by H_2 in the lump zone, and the FeO mass fraction entering the cohesive zone and dripping zone decreases, which makes the direct reduction process of FeO in the cohesive zone and dripping zone consume less heat and reduces the fuel consumption of the BF.



where: $\Delta_r G_m^\ominus$ is standard Gibbs free energy of reaction, J/mol; T is temperature, K.

2.3. Temperature Range from Cohesive Zone to 1273K

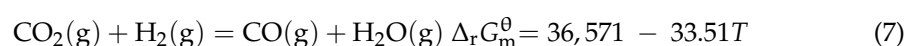
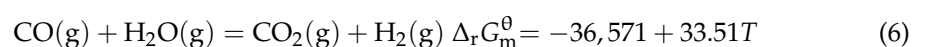
In this area, the iron-bearing burden is still in a solid state and contains a large amount of iron oxides that have not been reduced. H_2 reacts with these iron oxides, as shown in Equations (4) and (5).



Because the H_2 molecule is small, its diffusion capacity is much higher than that of CO, and the thermal conductivity of H_2 is much higher than that of CO [20]. Therefore, the heat transfer rate of hydrogen-rich reduction is faster, and the kinetic conditions of iron ore reduction are more favorable, so the reduction reaction proceeds faster [21,22]. Most of the steam generated in this area causes a gasification reaction with coke to regenerate H_2 . Therefore, the main role of H_2 at this stage is still to act as a carrier to accelerate the reaction, promote the chemical reaction between coke and iron ore, and have a relatively small impact on the heat change in this area.

2.4. Lower Than 1273 K

The gasification reaction rate of coke in this temperature region is lower than that in the high-temperature region, and H_2 reacts with various valence iron oxides to form H_2O , which cannot completely react with coke to convert into H_2 . H_2 in the gas partially replaces CO to reduce iron oxide, thus increasing the heat consumption of iron oxide reduction. There is also a water-gas shift reaction in this region (Equations (6) and (7)). In the standard state, the equilibrium transition temperature is about 1083 K. Above this temperature, H_2 reduces part of CO_2 to CO.



When the temperature is lower than the equilibrium transition temperature of the water-gas shift reaction, the thermodynamic reduction ability of CO exceeds that of H_2 . Since H_2 has a small atom and a large reaction rate constant, it preferentially reduces

iron oxide, but the H_2O generated after reduction is partially reduced to H_2 by CO. Kemppainen et al. [23] studied the effect of high H_2O concentration on the composition when reducing gas in the water-gas shift reaction at the upper part of the BF by using experimental methods, and pointed out that the magnetite formed in the reduction reaction at 673–723 K has a positive catalytic effect on the water-gas shift reaction (Equation (6)), which reduces the utilization rate of H_2 in the BF. However, Ono-Nakazato et al. [24] studied the effect of CO- H_2 on $FeO_{1.05}$ reduction at 1093 K and pointed out that the presence of water-gas shift reaction (Equation (7)) promoted the increase of reduction rate.

In general, the hydrogen enrichment of the BF increases the heat consumption in the tuyere area, which can be compensated by the measures of oxygen enrichment and high blast temperature. When the temperature is above 1273 K, the role of H_2 is mainly the catalytic reduction reaction, and the influence on heat is relatively low. However, when the temperature is lower than 1273 K, H_2 participates in the reduction of iron oxide and absorbs a large amount of heat, which reduces the lump zone heat and further affects the burden reduction and gas utilization rate. In order to alleviate this phenomenon, the BF top gas after CO_2 removal is usually heated and re-injected into the BF from the bottom of the furnace stack to improve the temperature of the lump zone and gas utilization rate [25,26].

3. Effect of H_2 on Blast Furnace Smelting

3.1. Effect of H_2 on Reduction Mechanism of Iron-Bearing Burden

After the hydrogen-rich smelting of BF, the reduction behavior of the sinter and pellets in the lump zone changed, and then the property of reduction disintegration changed. The fundamental reason for reduction disintegration is that hematite (Fe_2O_3) in the iron ore reduces to magnetite (Fe_3O_4) under low-temperature conditions, resulting in lattice transformation and volume expansion, causing lattice distortion to generate internal stress and fracture and disintegration [27–29]. Shen et al. [30] compared and analyzed the influence of H_2 and CO on the property of reduction disintegration of sinter, and pointed out that when H_2 replaces CO in the same amount, the volume fraction of H_2 increases from 0% to 12%, and the $RDI_{-3.15\text{ mm}}$ of sinter decreases by about 1~2%. This is mainly because the reduction ability of H_2 is weaker than that of CO at 773 K, which decreases the reduction degree and helps to inhibit the reduction disintegration of the sinter. However, when H_2 increases in the same amount and the volume fraction of CO, CO_2 , and N_2 decreases in the same proportion, the $RDI_{-3.15\text{ mm}}$ of sinter increases by about 1.5~2.5%, mainly because the total reducing gas (CO+ H_2) concentration increases with the increase of H_2 volume fraction, which promotes the occurrence of low-temperature reduction disintegration of sinter. Tian et al. [31] also studied the low-temperature reduction disintegration behavior of the sinter when H_2 replaces CO in the same amount, and found that the increase of H_2 volume fraction helps to inhibit the reduction disintegration phenomenon, and pointed out that the crack density of the sinter decreases sharply. However, Murakami et al. [32,33] pointed out that the reduction of CO mainly occurs near the surface particles of the sinter while the reduction of H_2 can diffuse into the sinter for reduction, which makes the low-temperature reduction disintegration of the sinter more serious. The disintegration mechanism is shown in Figure 1. This indicates that the effect of H_2 on the low-temperature reduction disintegration of the sinter is also related to the kinetic process of reduction.

The molecular size of H_2 (collision diameter 2.915×10^{-10} m) is less than the CO molecular size (collision diameter 3.590×10^{-10} m) [34]. At 1000 K, the interdiffusion coefficient of H_2 - H_2O is $7.330\text{ cm}^2/\text{s}$ and that of CO- CO_2 is $1.342\text{ cm}^2/\text{s}$ [30]. Since the molecular size of H_2 and H_2O is much smaller than that of CO and CO_2 , the reactants and products are more likely to diffuse to or leave the reaction interface in the pores of the iron ore. It can be seen from the kinetic model of the gas-solid reaction that diffusion is the limiting link of the reaction at higher temperatures. Therefore, the reduction of iron oxide with H_2 has more kinetic advantages than that with CO. Zuo et al. [35] pointed out that the reduction ability of H_2 is obviously stronger than that of CO at 1173 K. Cao et al. [36] studied that when the H_2 volume fraction in the reducing gas is 10%, the reduction degrees

of the sinter at 973, 1173, and 1273 K increases by 15.3%, 11.5%, and 11.4%, respectively, compared with that at the 0 H₂ volume fraction. The kinetic analysis shows that the initial stage of reduction is controlled by interfacial reaction, and the middle and late stage is controlled by internal diffusion and interfacial chemical reaction. After the volume fraction of H₂ increases, the reducing gas is more likely to diffuse to the iron ore surface, and at the same time, it is more likely to diffuse through the porous reduction product layer and then to the reduction reaction interface. Therefore, the internal diffusion resistance relatively decreases [37], and the chemical reaction resistance relatively increases.

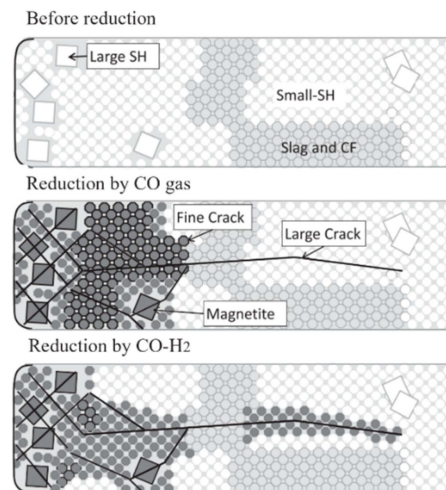


Figure 1. Reduction disintegration mechanism of sinter, adopted from [32]. SH: Skeletal hematite; CF: multi-component calcium ferrite.

After hydrogen-rich smelting in BF, the reduction of iron oxide is accelerated, and the mineral composition and microstructure at various temperatures are changed. Wang et al. [38] studied the reduction micromorphology of the sinter under a hydrogen-rich atmosphere and pointed out that under the condition of constant CO volume fraction, with the increase of H₂ volume fraction, the formation of a liquid phase in the sinter gradually tends to be good. Also, a good iron phase appears in the sinter, which is interconnected in a network and has obvious aggregation. When the volume fraction of (CO+H₂) is constant, increasing the volume fraction of H₂ is more conducive to the increase of the iron phase in the sinter. Abdelrahim et al. [39] and Kemppainen et al. [40] studied the effect of H₂-H₂O on the reduction of pellets and pointed out that H₂-H₂O in the gas phase has a positive effect on the reduction. Compared with CO-CO₂-N₂, metal iron can be formed at the periphery and core of pellets at a lower temperature, and increasing the H₂ volume fraction increases its porosity and surface area. In the study of the expansion behavior of pellets under different atmospheres, it was also found that there are some large particles of iron oxide that are not reduced during the reduction of CO, and the iron phase is small fragments after reduction. During H₂ reduction, the reduction of iron oxide is relatively complete, no large particles of iron oxide are found, and the iron phase after reduction is relatively dense [35]. This is because the reaction rate of H₂ and iron oxide is fast, which promotes the formation of a large number of iron crystal nuclei, and the adjacent metal iron grains gather to form an iron layer, filling the cracks and pores caused by volume expansion, and making the pellet structure compact and shrink [41–44]. This also enables H₂ reduction to effectively inhibit the abnormal expansion caused by the growth of iron whiskers [45,46]. According to the first principle calculation results based on density functional theory and the research results of molecular dynamics theory, when FeO is reduced by CO, the precipitated iron on the surface of FeO grows into a whisker structure, while when FeO is reduced by H₂, the precipitated iron on the surface of FeO grows into a dense layered structure (Figure 2) [42,47]. The different morphologies of

the iron precipitated during the reduction of FeO by CO and H₂ are consistent with the macroscopic experimental results.

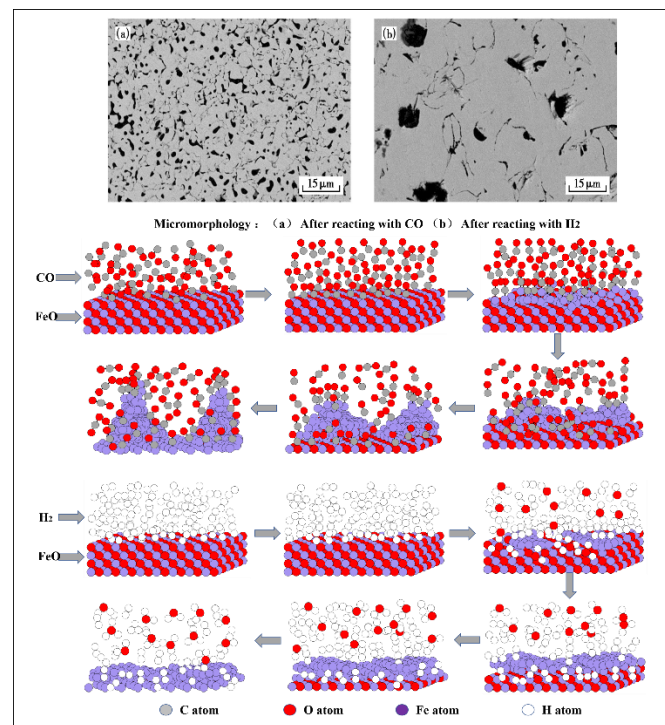


Figure 2. Microstructure of iron oxide reacting with CO and H₂, adapted from [42,47]. (a) After reacting with CO; (b) After reacting with H₂.

3.2. Effect of H₂ on Gasification Behavior and Structure Evolution of Coke

The gasification reaction of coke is one of the important reasons for the deterioration of coke property. After hydrogen-rich smelting in the BF, H₂ reduces iron ore to generate H₂O, which gasifies with coke, thus changing the gasification reaction behavior and structure evolution process of coke in the BF. At present, researchers have conducted some research work on the gasification reaction behavior of H₂O and coke. According to the literature [48–54], a comparative study on the thermodynamic and kinetic behaviors of the solution loss reaction of coke with CO₂ and H₂O found that the initial reaction temperature of coke with H₂O is lower than that of coke with CO₂ (Figure 3). The internal diffusion condition and interface reaction condition of coke gasification in H₂O are better than that of CO₂, and the difference in diffusion property is greater than that of interface reaction property. Moreover, the chemisorption capacity of CO₂ on coke surface is weaker than that of H₂O. The activation energies of internal diffusion and interface reaction of coke with H₂O decrease by 80.36 kJ/mol and 36.97 kJ/mol, respectively, compared with that of coke with CO₂. The limiting link in the reaction with H₂O is that the area of the interface reaction is larger than that of CO₂ (Figure 4). Lan et al. [55] also studied the kinetics of coke gasification under an N₂-CO-CO₂-H₂-H₂O atmosphere and pointed out that with the increase of the volume fraction of H₂O, the area controlled by the interfacial reaction at each temperature gradually increases. Also, the higher the volume fraction of H₂O, the greater the increase of the area controlled by the interfacial reaction with the increase in temperature. Zhang et al. [56] studied the effect of H₂ on the gasification kinetics of coke in CO₂-CO-N₂ atmosphere by using a thermogravimetric analyzer. The study pointed out that H₂ can obviously promote the gasification reaction of coke, and the addition of H₂ can reduce the apparent activation energy of the coke gasification reaction. Haapakan-gas et al. [57] found that partial replacement of CO/CO₂ with H₂/H₂O can significantly

improve the solution rate of coke at 1373 K, and the effect of the solution rate increase is related to temperature, reaching the highest at 1373 K.

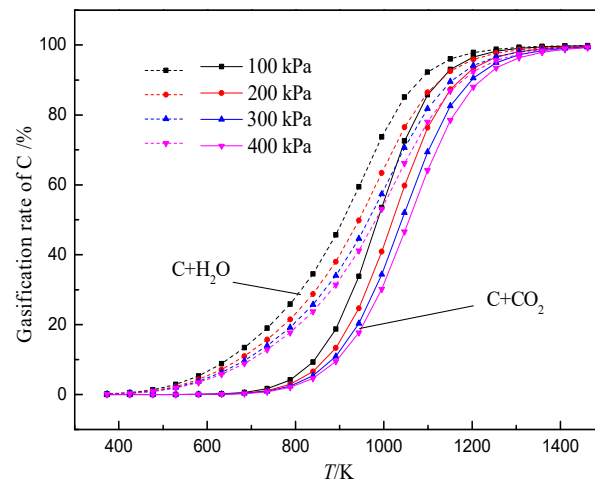


Figure 3. Relationships between gasification rate and temperature of carbon reacting with CO_2 and H_2O , adopted from [55], with permission from Elsevier 2018.

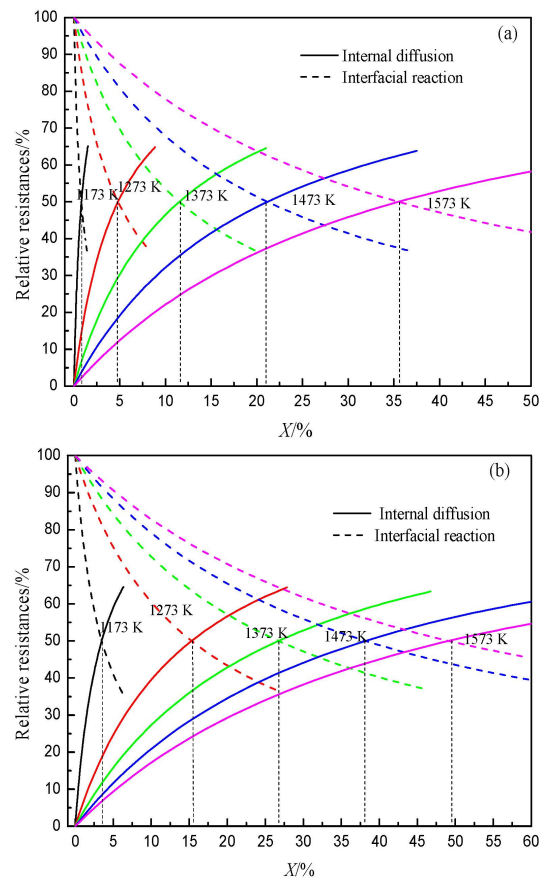


Figure 4. Relationship between reaction ratio and relative resistances at different temperatures, adopted from [49]. (a) Coke gasification by CO_2 ; (b) Coke gasification by H_2O .

Due to the great differences in the thermodynamic and kinetic behaviors of the reaction of coke with H_2O and CO_2 , the pore structure of coke after the reaction also changes greatly. Research indicates that [58–61], compared with the reaction of coke and CO_2 , the reaction of coke and H_2O mainly occurs on the surface of particles. When coke reacts with CO_2 and H_2O , the large pores at the edge increase by 66.98% and 94.01%, respectively, compared

with that before the reaction. When the solution loss rate of coke increases by 1%, the strength after reaction with CO_2 and H_2O decreases by 1.200% and 0.786%, respectively. The influence of H_2O on the strength of coke is less than that of CO_2 . Guo [62] pointed out that CO_2 and H_2O have a selective effect on the solution of different optical tissues. Compared with CO_2 , H_2O can promote the gasification of optical tissues with strong gasification resistance. Wang et al. [63] studied the influences of H_2O on the reactivity and structural evolution of coke. The reactivity of coke increases with the increase of H_2O volume fraction, while the strength decreases. H_2O can promote the formation of pores in coke and also increase the graphitization degree of coke. Xu et al. [64] studied the gasification reaction and structural change of coke under an $\text{H}_2\text{O}/\text{CO}_2$ atmosphere and obtained the microstructure before and after the coke reaction under different conditions. As shown in Figure 5, the study pointed out that H_2O has greater damage to the coke structure than CO_2 . During the gasification reaction between coke and H_2O , the pore wall of coke is eroded, the pore diameter of coke expands rapidly, the pore depth further expands, and even cracks are generated, and the pore wall becomes thin or even becomes damaged, resulting in hole connection, thereby forming a channel for the reaction gas. The research conclusions in some studies [63,64] are inconsistent with those in the literature [58–61], which is mainly caused by the difference in experimental conditions. The literature [58–61] compares the strength changes of coke after reacting with CO_2 and H_2O , respectively, under the same solution loss rate, and it is found that the influence of H_2O on the strength of coke is weaker than that of CO_2 . The literature [63,64] compares the coke strength changes at the same time as when coke reacts with CO_2 and H_2O , respectively. Because the reaction rate of coke and H_2O is larger than that of CO_2 , the reaction loss rate of coke and H_2O is higher, and the degradation effect of H_2O on coke strength is stronger than that of CO_2 .

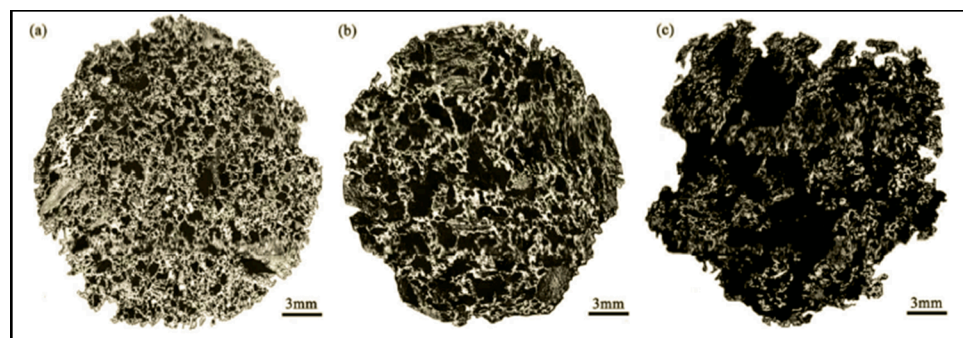


Figure 5. Panoramic images of coke under different reaction conditions, adopted from [64], with permission of American Chemical Society, 2017. (a) Unreacted coke; (b) Coke reacted with pure CO_2 ; (c) Coke reacted with pure H_2O .

In the BF, the iron oxide is reduced with rising high-temperature reducing gas (CO and H_2) to generate a large amount of CO_2 and H_2O , which can react with coke to generate CO and H_2 again. This shows that in the actual production process of BF, CO_2 and H_2O participating in the coke gasification reaction mainly come from the reduction of iron oxide, and the concentration depends on the reduction degree of iron oxide. This indicates that there is a coupling behavior between ore reduction and coke gasification in the BF (hereinafter referred to as “ore-coke coupling reaction”). The starting temperature of the coke gasification reaction is about 1173 K. At this time, the gasification reaction rate is low. With the increase in temperature, the gasification reaction rate of coke gradually increases. After the coke begins to gasify, the reduction rate of iron ore at various temperatures directly affects the strength of the ore-coke coupling reaction and the gasification behavior of coke. Sun et al. [65] studied the solution loss characteristics of coke and sinter during the coupling reaction. It was found that the solution loss rate of coke is positively correlated with the reduction degree of sinter. After the coupling reaction, the optical anisotropy index, average pore diameter, and porosity of coke increase significantly. According to the

research of Lan [66,67], under the N_2 - CO - H_2 atmosphere, with the increase of H_2 volume fraction, the temperature range with the largest increase in the gasification rate of coke gradually moves to the low-temperature zone. When the H_2 volume fraction increases from 5% to 10%, the gasification rate of coke increases the most. In the absence of H_2 , the total amount of CO_2 produced by the reduction of iron oxide and the CO_2 consumption in the process of coke gasification is less in the low-temperature region. With the increase in temperature, the total amount of CO_2 produced by the reduction of iron oxide and the amount of CO_2 consumed by coke gasification gradually increase. In the case of H_2 , a large amount of iron oxide is reduced in the low-temperature zone, producing a large amount of CO_2 and H_2O . Compared with the absence of H_2 , the gasification rate of coke is improved to a certain extent. Although the total amount of CO_2 and H_2O produced by the reduction of iron oxide in the high-temperature zone decreases with the increase in temperature, the gasification amount of coke still greatly increases due to the presence of H_2O . The gasification reaction rate of H_2O and coke is much higher than that of CO_2 and coke. This indicates that the presence of H_2 intensifies the gasification of coke (Figure 6), and with the increase of H_2 volume fraction, the reduction of iron oxide tends to proceed in the low-temperature region, while the volume fraction of CO_2 and H_2O produced in the high-temperature region decreases. This increases the porosity of coke in the low-temperature zone but decreases the internal porosity of coke in the high-temperature zone (Figure 7), which helps to improve the strength of coke after a high-temperature reaction.

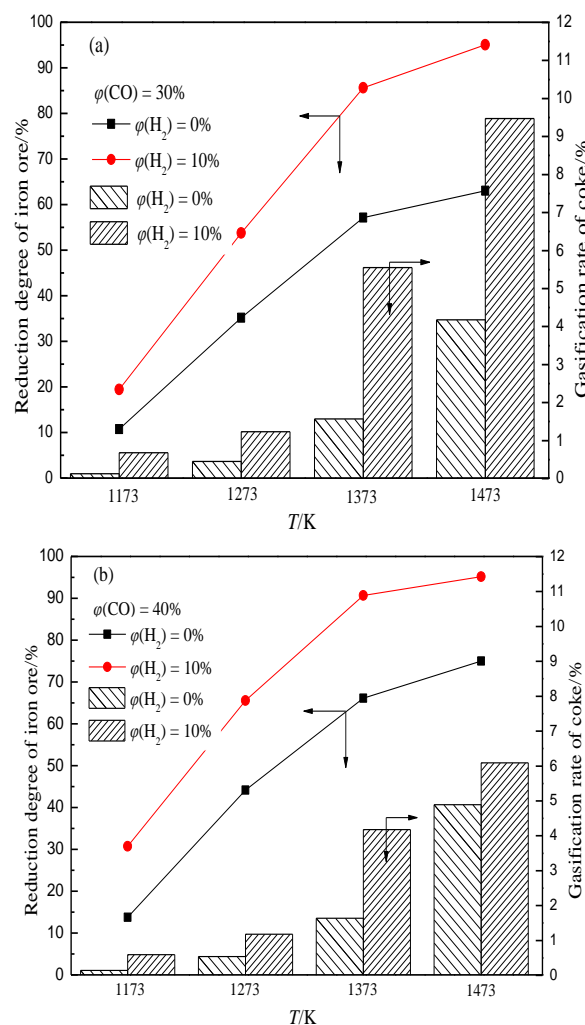


Figure 6. Effects of H_2 on reduction degree of iron ore and coke gasification rate under different conditions, adopted from [67]. (a) $\phi(CO) = 30\%$; (b) $\phi(CO) = 40\%$.

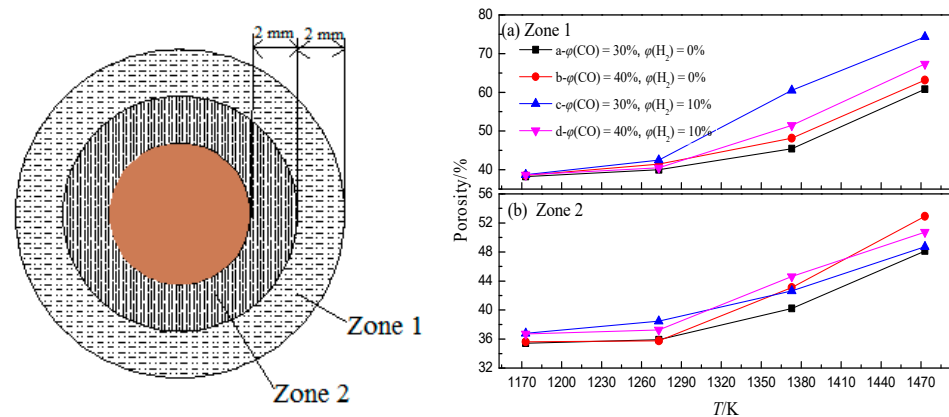


Figure 7. Porosity of coke zone 1 and zone 2 under different conditions, adopted from [67]. (a) Zone 1; (b) Zone 2.

3.3. Effect of H_2 on Cohesive Zone of Blast Furnace

The softening and melting of the iron-bearing burden in the BF is mainly due to the gradual increase of wüstite mass fraction with the increase of temperature, which forms a large number of low melting point compounds with the minerals in the slag, and makes the slag and iron gradually separate and drip. Research has pointed out that [68–71], the increase of H_2 volume fraction in gas can accelerate the reduction of iron oxide, and a large amount of wüstite forms in the burden at a lower temperature. With the increase in temperature, the burden is rapidly reduced to metal iron, which changes the melting state of the slag and iron in the cohesive zone. Lan et al. [72], Li et al. [73], and Yan et al. [74] found that with the increase of H_2 volume fraction under an N_2 -CO- H_2 atmosphere, the softening start temperature of burden decreases and the softening end temperature increases, which widens the softening temperature range, and the melting temperature range of slag iron decreases greatly, which improves the permeability of the cohesive zone (Figure 8). The research of Yang and Du also obtained similar conclusions [75,76].

Lan et al. [73] carried out a detailed analysis of this change mechanism and pointed out that after hydrogen enrichment, the burden is greatly reduced before 1473 K so that the amount of wüstite entering the cohesive zone is very small, and the low melting point materials in the burden decrease. At the same time, the reduced metal iron phase has a strong deformation resistance, so that $T_{10\%}$ (softening start temperature, that is, the temperature when the burden contracted by 10%) gradually increases. With the increase of H_2 volume fraction in the gas, a large amount of wüstite in the primary slag is further reduced to the metal iron phase before melting, so that the mass fraction of low melting point substances in the slag decrease, the melting point of the slag increases, and the slag amount decreases, which has little impact on the permeability of the stock column. Furthermore, the T_s (melting start temperature, that is, the temperature when the pressure difference starts to rise steeply) significantly increases. After the melting point of the slag rises, the ash stratification on the coke surface due to the gasification reaction cannot be timely fused with the slag, the “active” point on the coke surface cannot be timely updated, and the carburizing reaction of metal iron is inhibited, resulting in an increase in T_d (dripping temperature, that is, the temperature when the burden starts to drip). With the increase in temperature, the carburizing rate of the metal iron phase increases sharply, and the carburizing amount required for the melting of the metal iron phase also decreases gradually. At the same time, the graphitization degree of coke increases with the increase in temperature, which promotes the occurrence of carburizing reaction. These conditions make the metal iron rapidly carburized and melted in a small temperature range. Therefore, the increase in T_d is relatively small. This makes the temperature range of the melting zone narrower, and the comprehensive permeability of the cohesive zone of the BF greatly improves. Higuchi et al. [77] also confirmed this view in the process

of studying the injection of coke oven gas into BF, pointing out that the increase in coke oven gas decreases the corrosion degree of slag to coke during the reduction process and improves the permeability of stock column.

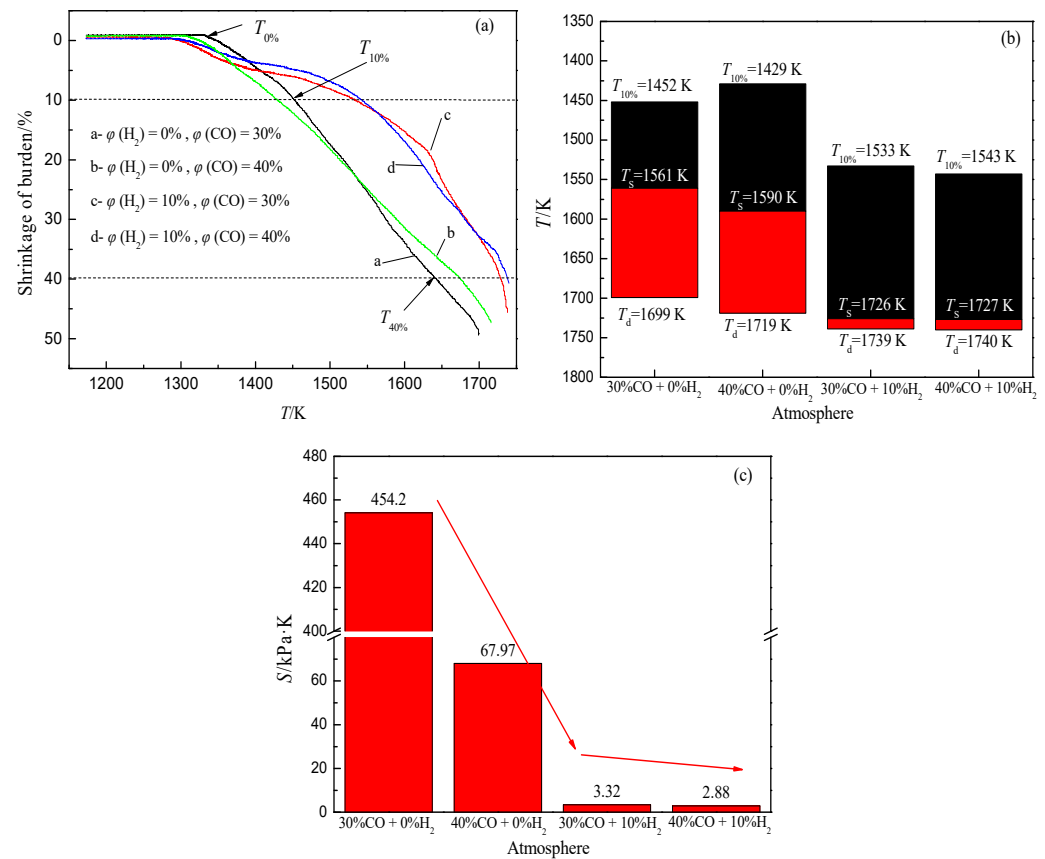


Figure 8. Change of softening-melting property of burden, adopted from [72], with permission from Elsevier, 2020. (a) Relationship between shrinkage and temperature; (b) Characteristic temperature of cohesive zone; (c) Permeability index of cohesive zone under different atmospheres.

4. Problems to Be Further Studied in Hydrogen-Rich Smelting of Blast Furnace

In addition to the above effects and changes, many aspects of hydrogen-rich smelting of BF need further study.

(1) Utilization rate of hydrogen and degree of substitution for direct reduction

The steam generated in the process of reduction of iron oxide by H₂ has a lower reaction temperature and higher reaction rate with coke, which makes more steam change into H₂ again. That is, part of H₂ only plays a role of accelerating reaction or intermediation, and its amount is related to temperature and reaction conditions. In addition, there is also a water-gas shift reaction in the lump zone of BF, and H₂ and CO₂ are generated in the upper part of the BF, which plays a key role in the overall H₂ and CO utilization rate, and also affects the economy of hydrogen utilization, the composition and calorific value of the furnace top gas, and thus the energy balance of the whole plant. At present, there are few studies on the basic thermodynamic and kinetic data of these reactions, and the reaction degree of these reactions in the BF cannot be accurately simulated and predicted, which further affects the hydrogen utilization rate in the gas and the accurate determination of the degree of substitution for direct reduction.

(2) Study on combustion behaviors in raceway

When the BF is not rich in hydrogen, the tuyere area of the BF is mainly the combustion reaction between pulverized coal and oxygen. When the BF is rich in hydrogen, there is a lot

of H₂, hydrocarbons, and other substances in the tuyere area, which makes the combustion more complicated. Whether hydrogen participates in the combustion reaction before gasification, whether the combustion of hydrocarbons has an impact on the combustion of pulverized coal, whether the combustion of pulverized coal will be delayed and more incomplete, the determination of the appropriate injection amount of pulverized coal and the appropriate oxygen enrichment rate during hydrogen-rich smelting, and the combustion temperature of hydrogen can reach 3200 K, what are the requirements for the injection equipment and tuyeres? These problems need further study.

(3) Control of gas flow distribution in BF

When the proportion of hydrogen in the gas increases, the raceway may become smaller while maintaining the same theoretical combustion temperature of the raceway and the amount of hearth gas [78]. At the same time, in order to compensate for the heat loss of the lump zone, the heated reduction gas is usually injected into the furnace stack. Research shows that [79], the penetration depth of H₂ is limited, mainly concentrated in the furnace wall area, rising with the gas flow, and the injected gas may not reach the center of the BF. This indicates that after hydrogen enrichment, the uneven distribution of gas in the BF increases, which makes the reduction state of iron-bearing burden and the degree of coke deterioration unevenly distribute [80]. Therefore, in order to improve the utilization efficiency of reducing gas in BF, it is necessary to increase the penetration depth of hydrogen-rich gas and control the gas flow distribution in the BF.

(4) Operation optimization of BF

After the BF is injected with hydrogen-rich gas, the above-mentioned series of changes are brought to the smelting process of the BF, which makes the appropriate operating parameters in the smelting process of the BF different from those of the traditional BF [81,82]. Therefore, after the hydrogen-rich smelting of BF, the BF operation needs to be further optimized. The main directions are as follows:

- (1) The reduction mechanism of iron ore changes and the requirements of BF on the metallurgical properties of iron ore need to be re-formulated.
- (2) The coke ratio of BF decreases, and the gasification behaviors of coke change. The requirements of BF on the metallurgical properties of coke and the evaluation method need to be re-formulated.
- (3) The permeability of the cohesive zone improves significantly. The formation process of slag-iron in the cohesive zone and the metallurgical behavior of the slag-coke-iron interface need to be further studied.
- (4) As the temperature of the gas on the top of the BF decreases and the steam volume fraction increases, the impact on the dust removal system and the utilization of the gas need to be deeply considered.
- (5) The gas composition distribution is uneven, and the inhibition effects of the cohesive zone permeability on the BF production decrease. Therefore, the charging systems of the BF need to be adjusted and optimized to match the hydrogen-rich smelting.

5. Conclusions

Hydrogen-rich smelting of BF is very important for reducing energy consumption and CO₂ emission of ironmaking system and is one of the important directions of green and low-carbon development of iron and steel enterprises.

After H₂ enters the BF, the heat consumption in the tuyere area increases. At the same time, the combustion and cracking of hydrocarbons increase the gas volume and decrease the theoretical combustion temperature. It needs to take measures of oxygen enrichment and high blast temperature to compensate. When the temperature is above 1273 K, the effect of H₂ on heat is small. When the temperature is lower than 1273 K, H₂ participates in the reduction process of iron oxide to absorb a large amount of heat, so that the heat of the lump zone decreases.

The reduction kinetic condition of H₂ on iron oxide is better than that of CO, which makes the reduction rate of iron ore increase and the internal diffusion resistance decrease after hydrogen enrichment in BF. During the reduction process, a large number of iron crystal nuclei are promoted to form, so that adjacent metal iron grains gather to form an iron layer. Hydrogen-rich smelting in BF changes the deterioration mechanism of coke, so that a large amount of iron oxides is reduced in the low-temperature area, and the total amount of H₂O and CO₂ produced in the high-temperature area decreases. Moreover, H₂O tends to be gasified on the surface of coke and has little impact on the strength of coke in the high-temperature area. After hydrogen enrichment, the permeability of the cohesive zone increases significantly, and the carburizing rate of metallic iron becomes the limiting factor of the cohesive zone.

After the hydrogen enters the BF, it brings some changes to the BF smelting, and the following aspects need to be further studied: (1) The utilization rate of hydrogen and degree of substitution for direct reduction. (2) Combustion behavior of fuel in the raceway. (3) Control of gas flow distribution in BF. (4) Operation optimization of BF.

Author Contributions: Conceptualization, C.L. and Y.H.; methodology, S.Z. and R.L.; investigation, J.S.; data curation, C.L. and Y.H.; writing—original draft preparation, C.L. and S.Z.; writing—review and editing, R.L. and Q.L. All authors have read and agreed to the published version of the manuscript.

Funding: This research was funded by [National Natural Science Foundation of China] grant number [52204344], [Natural Science Foundation of Hebei Province] grant number [E2021209046, 22374003D], [Tangshan Science and Technology Planning Project] grant number [21130209C], and [Basic Scientific Research Business Expenses of Hebei Provincial Colleges and Universities] grant number [JQN2021015].

Conflicts of Interest: The authors declare no conflict of interest.

References

1. Wei, Y.J. Technology prospect for achieving the long term goal of reducing CO₂ emission from iron and steel. *World Met. Guide* **2020**.
2. Tang, J.; Chu, M.S.; Li, F.; Feng, C.; Liu, Z.G.; Zhou, Y.S. Development and progress on hydrogen metallurgy. *Int. J. Miner. Metall. Mater.* **2020**, *27*, 713–723. [[CrossRef](#)]
3. Su, Y.H. Development status and suggestions of hydrogen metallurgy in China's iron and steel industry. *China Metall. News* **2021**.
4. Gao, Y.M. Development status and future prospect of hydrogen metallurgy abroad. *Metall. Manag.* **2020**, *20*, 4–14.
5. Gao, J.J.; Zhu, L.; Ke, J.C.; Huo, X.F.; Qi, Y.H. Industrialized application of hydrogen-rich gas injection into blast furnace of Jinnan Steel. *Iron Steel* **2022**, *57*, 42–48.
6. Zhang, F.M.; Cheng, X.F.; Yin, G.Y.; Cao, C.Z. Development of low-carbon green ironmaking technology at home and abroad. *Ironmaking* **2021**, *40*, 1–8.
7. Pan, C.C.; Pang, J.M. Development trace and application prospect of hydrogen metallurgy technology. *China Metall.* **2021**, *31*, 73–77.
8. Wang, G.D.; Chu, M.S. Green steelmaking technology with low carbon emission. *Sci. Technol. Guide* **2020**, *38*, 68–76.
9. China Business Intelligence Network. Ranking of Pig Iron Production in China in 2021: Hebei Ranks First. Available online: <https://baijiahao.baidu.com/s?id=1724970607796914435&wfr=spider&for=pc,2022-02-17> (accessed on 30 August 2022).
10. Kong, L.B.; Guo, P.M.; Wang, L.; Zhao, P. Reduction behavior of hydrogen injected in blast furnace. *Sinter. Pelletizing* **2020**, *45*, 1–4.
11. Che, Y.M.; Cao, L.X.; Liu, J.Z. Large scale hydrogen production and its application and prospect in iron and steel industry. *China Metall.* **2022**, *32*, 1–7.
12. Zhang, X.H.; Li, H.F.; Xu, W.R.; Zou, Z.S. Development of a mathematical model of raceway adiabatic flame temperature in hydrogen-rich blast furnace. *J. Mater. Metall.* **2022**, *21*, 31–36.
13. Murai, R.; Sato, M.; Ariyama, T. Design of innovative blast furnace for minimizing CO₂ emission based on optimization of solid fuel injection and top gas recycling. *ISIJ Int.* **2004**, *44*, 2168–2177. [[CrossRef](#)]
14. Meng, X.L.; Zhang, F.M.; Wang, W.Q.; Li, L. Analysis of pulverized coal and natural gas Injection in 5 500 m³ blast furnace in Shougang Jingtang. In Proceedings of the AISTech 2015, Cleveland, OH, USA, 4–7 May 2015; p. 946.
15. Silaen, A.K.; Okosun, T.; Zhao, J.Q. Study of injection natural gas into blast furnace. In Proceedings of the AISTech, Pittsburg, PA, USA, 16–19 May 2016; p. 595.
16. Jampani, M.; Pistorius, P.C. Increased use of natural gas in blast furnace ironmaking: Methane reforming. In Proceedings of the AISTech, Pittsburg, PA, USA, 16–19 May 2016; p. 573.
17. Guo, T.L.; Chu, M.S.; Liu, Z.G.; Tang, J.; Yagi, J.I. Mathematical Modeling and exergy analysis of blast furnace operation with natural gas injection. *Steel Res. Int.* **2013**, *84*, 333–343. [[CrossRef](#)]

18. Qie, Y.N.; Lyu, Q.; Lan, C.C.; Zhang, S.H.; Liu, R. Effect of H₂ addition on process of primary slag formation in cohesive zone. *J. Iron Steel Res. Int.* **2022**, *27*, 132–140. [[CrossRef](#)]
19. Qie, Y.N.; Lyu, Q.; Liu, X.J.; Li, J.P.; Lan, C.C.; Zhang, S.H.; Yan, C.J. Effect of hydrogen addition on softening and melting reduction behaviors of ferrous burden in gas-injection blast furnace. *Metall. Mater. Trans. B* **2018**, *49*, 2622–2632. [[CrossRef](#)]
20. Lyu, Q.; Qie, Y.N.; Liu, X.J.; Lan, C.C.; Li, J.P.; Liu, S. Effect of hydrogen addition on reduction behavior of iron oxides in gas-injection blast furnace. *Thermochim. Acta* **2017**, *648*, 79–90. [[CrossRef](#)]
21. Yi, L.Y.; Huang, Z.C.; Peng, H.; Jiang, T. Action rules of H₂ and CO in gas-based direct reduction of iron ore pellets. *J. Cent. S. Univ.* **2012**, *19*, 2291–2296. [[CrossRef](#)]
22. Jin, Y.L.; He, Z.J.; Guan, Z.G.; Zhang, J.H. Practice and theoretical analysis about effect of H₂ content on ironmaking process. *Iron Steel* **2011**, *46*, 15–18.
23. Kemppainen, A.; Alatarvas, T.; Iljana, M.; Haapakangas, J.; Mattila, O.; Paananen, T.; Fabritius, T. Water-gas shift reaction in an olivine pellet layer in the upper part of blast furnace shaft. *ISIJ Int.* **2014**, *54*, 801–809. [[CrossRef](#)]
24. Ono-Nakazato, H.; Yonezawa, T.; Usui, T. Effect of water-gas shift reaction on reduction of iron oxide powder packed bed with H₂-CO mixtures. *ISIJ Int.* **2003**, *43*, 1502–1511. [[CrossRef](#)]
25. Xue, Q.G.; Yang, F.; Zhang, X.X.; Wang, J.S.; Zuo, H.B.; Jiang, Z.Y.; She, X.F.; Wang, G. Development of an oxygen blast furnace and its research progress in University of Science and Technology Beijing. *Chin. J. Eng.* **2021**, *43*, 1579–1591.
26. Zhang, J.L.; Wang, G.W.; Shao, J.G.; Zuo, H.B. Comprehensive mathematical model and optimum process parameters of pitrogen free blast furnace. *J. Iron Steel Res. Int.* **2014**, *21*, 151–158. [[CrossRef](#)]
27. Zhang, Z.H.; Xu, K.Q.; Xing, X.D.; Lu, H.H.; Quan, J. Research progress of influence factors on low-temperature reduction degradation. *J. Iron Steel Res.* **2021**, *33*, 453–460.
28. Lei, C.; Wei, Y.G. Pulverization of iron ore sinter in low temperature reduction process. *Chin. J. Process Eng.* **2015**, *15*, 284–288.
29. Pimenta, H.P.; Seshadri, V. Characterisation of structure of iron ore sinter and its behaviour during reduction at low temperatures. *Ironmak. Steelmak.* **2002**, *29*, 169–174. [[CrossRef](#)]
30. Shen, F.M.; Jiang, X.; Wei, G.; Zheng, H.Y.; Mu, L. Effect of hydrogen-enriched gas on reducibility and reduction-disintegration of sinters. *China Metall.* **2014**, *24*, 2–5.
31. Tian, Y.; Lyu, Q.; Liu, X.J.; Chen, S.J.; Sun, Y.Q. Study on reduction and disintegration behavior of sinter under CO-H₂-CO₂-N₂ conditions. *Sinter. Pelletizing* **2016**, *41*, 1–5.
32. Murakami, T.; Kamiya, Y.; Kodaira, T.; Kasai, E. Reduction disintegration behavior of iron ore sinter under high H₂ and H₂O conditions. *ISIJ Int.* **2012**, *52*, 1447–1453. [[CrossRef](#)]
33. Murakami, T.; Kodaira, T.; Kasai, E. Reduction and disintegration behavior of sinter under N₂-CO-CO₂-H₂-H₂O gas at 773K. *ISIJ Int.* **2015**, *55*, 1181–1187. [[CrossRef](#)]
34. Zou, Z.S.; Wang, C. On hydrogen-enriching gas reform for pre-reduction in smelting reduction iron-making process. *Iron Steel* **2007**, *42*, 17–20.
35. Zuo, X.J.; Wang, J.S.; An, X.W.; She, X.F.; Xue, Q.G. Reduction behaviors of pellets under high reduction potential. *Iron Steel Vanadium Titan.* **2013**, *34*, 46–53.
36. Cao, K.; Wang, W.; Li, X.W.; Zhu, H.Y.; Xue, Z.L.; Chen, L.K. H₂-rich reduction kinetics of iron ore sinter. *Chin. J. Process Eng.* **2015**, *15*, 1024–1028.
37. Liang, Z.K. *Study on Gas-Based Reduction and Accompanying*; Central South University: Changsha, China, 2013.
38. Wang, Y.; He, Z.J.; Zhan, W.L.; Zhu, H.B.; Zhang, J.H.; Pang, Q.H. Reduction behavior of iron-bearing burdens in hydrogen-rich steam. *Iron Steel* **2020**, *55*, 34–40.
39. Abdelrahim, A.; Iljana, M.; Omran, M.; Vuolio, T.; Bartusch, H.; Fabritius, T. Influence of H₂-H₂O content on the reduction of acid iron ore pellets in a CO-CO₂-N₂ reducing atmosphere. *ISIJ Int.* **2020**, *60*, 2206–2217. [[CrossRef](#)]
40. Kemppainen, A.; Mattila, O.; Heikkinen, E.P.; Paananen, T.; Fabritius, T. Effect of H₂-H₂O on the reduction of olivine pellets in CO-CO₂ gas. *ISIJ Int.* **2012**, *52*, 1973–1978. [[CrossRef](#)]
41. Wang, Z.C.; Chu, M.S.; Liu, Z.G.; Chen, S.Y.; Xue, X.X. Effect of temperature and atmosphere on pellets reduction swelling index. *J. Iron Steel Res. Int.* **2012**, *19*, 7–12. [[CrossRef](#)]
42. Wang, Z.C.; Chu, M.S.; Tang, J.; Xue, X.X. Effects of reducing atmosphere and gangue composition on reduction swelling of oxidized pellets. *J. Northeast. Univ.* **2012**, *33*, 94–97.
43. Li, W.; Fu, G.Q.; Chu, M.S.; Zhu, M.Y. Effect of reducing conditions on swelling behavior and mechanism of Hongge vanadium titanomagnetite-oxidized pellet with hydrogen-rich gases. *Int. J. Hydrogen Energy* **2017**, *42*, 24667–24674. [[CrossRef](#)]
44. Guo, Y.F.; Liu, K.; Liu, Y.J.; Chen, F.; Wang, S.; Zheng, F.Q. Research progress on reduction swelling mechanism and influencing factors of iron ore pellets. *Iron Steel* **2021**, *56*, 9–15.
45. Hayashi, S.; Iguchi, Y. Influence of several condition on abnormal swelling of hematite pellets during reduction with H₂-CO gas mixtures. *Ironmak. Steelmak.* **2013**, *32*, 353–358. [[CrossRef](#)]
46. Long, H.M.; Wang, H.T.; Di, Z.X.; Chun, T.J.; Liu, Z.G. Influence of hydrogen-enriched atmosphere under coke oven gas injection on reduction swelling behaviors of oxidized pellet. *J. Cent. South Univ.* **2016**, *23*, 1890–1898. [[CrossRef](#)]
47. Wei, J. *Research on the Mechanism of Precipitated Iron Morphology Difference During FeO Reduction Process by CO and H₂*; Chongqing University: Chongqing, China, 2018.

48. Chang, Z.Y.; Wang, P.; Zhang, J.L.; Jiao, K.X.; Zhang, Y.Q.; Liu, Z.J. Effect of CO₂ and H₂O on gasification dissolution and deep reaction of coke. *Int. J. Miner. Metall. Mater.* **2018**, *25*, 1402–1411. [[CrossRef](#)]
49. Lan, C.C.; Zhang, S.H.; Liu, X.J.; Liu, R.; Lyu, Q. Kinetic behaviors of coke gasification with CO₂ and H₂O. *ISIJ Int.* **2021**, *61*, 167–173. [[CrossRef](#)]
50. Wang, P.; Zhang, Y.Q.; Long, H.M.; Wei, R.F.; Yu, S.C. Degradation behavior of coke reacting with H₂O and CO₂ at high temperature. *ISIJ Int.* **2017**, *57*, 643–648. [[CrossRef](#)]
51. Guo, W.T.; Xue, Q.G.; Liu, Y.L.; Guo, Z.C.; She, X.F.; Wang, J.S.; Zhao, Q.Q.; An, X.W. Kinetic analysis of gasification reaction of coke with CO₂ or H₂O. *Int. J. Hydrogen Energy* **2015**, *40*, 13306–13313. [[CrossRef](#)]
52. Zhao, Q.Q.; Xue, Q.G.; She, X.F.; Wang, H.; Wang, J.S. Study on solution loss reaction kinetics of coke with H₂O and CO₂. *Chin. J. Process Eng.* **2012**, *12*, 790–795.
53. Wang, P.; Zhang, Y.Q.; Li, J.X.; Long, H.M.; Meng, Q.M.; Yu, S.C. Effect of CO₂ and H₂O on solution loss reaction of coke. *Chin. J. Process Eng.* **2016**, *16*, 138–143.
54. Numazawa, Y.; Hara, Y.; Matsukawa, Y.; Matsushita, Y.; Aoki, H.; Shishido, T.; Okuyama, N. Kinetic modeling of CO₂ and H₂O gasification reactions for metallurgical coke using a distributed activation energy model. *ACS Omega* **2021**, *6*, 11436–11446. [[CrossRef](#)]
55. Lan, C.C.; Lyu, Q.; Liu, X.J.; Jiang, M.F.; Qie, Y.N.; Zhang, S.H. Thermodynamic and kinetic behaviors of coke gasification in N₂-CO-CO₂-H₂-H₂O. *Int. J. Hydrogen Energy* **2018**, *43*, 19405–19413. [[CrossRef](#)]
56. Zhang, H. Gasification of metallurgical coke in CO₂-CO-N₂ with and without H₂. *Chem. Eng. J.* **2018**, *347*, 440–446. [[CrossRef](#)]
57. Haapakangas, J.; Suopajarvi, H.; Iljana, M.; Kempainen, A.; Mattila, O.; Heikkinen, E.P.; Samuelsson, C.; Fabritius, T. Coke reactivity in simulated blast furnace shaft conditions. *Metall. Mater. Trans. B* **2016**, *47*, 2357–2370. [[CrossRef](#)]
58. Wang, P.; Yu, S.C.; Long, H.M.; Wei, R.F.; Meng, Q.M.; Zhang, Y.Q. Microscopic study on the interior and exterior reactions of coke with CO₂ and H₂O. *Ironmak. Steelmak.* **2017**, *44*, 595–600. [[CrossRef](#)]
59. Shin, S.M.; Jung, S.M. Gasification effect of metallurgical coke with CO₂ and H₂O on the porosity and macrostrength in the temperature range of 1100 to 1500 °C. *Energy Fuels* **2015**, *29*, 6849–6857. [[CrossRef](#)]
60. Zhang, Y.Q. *Fundamental Study on Degradation Behavior of Coke with H₂O and CO₂*; Anhui University of Technology: Hefei, China, 2016.
61. Guo, W.T.; Wang, J.S.; She, X.F.; Xue, Q.G.; Guo, Z.C. Pore structure and high-temperature compressive strength of gasified coke with CO₂ and steam. *J. Fuel Chem. Technol.* **2015**, *43*, 654–662.
62. Guo, W.T. *The Influence of the Coke Microstructure on the Reaction Behavior and Performance in the Blast Furnace*; University of Science and Technology Beijing: Beijing, China, 2016.
63. Wang, W.; Dai, B.W.; Xu, R.S.; Schenk, J.; Wang, J.; Xue, Z.L. The effect of H₂O on the reactivity and microstructure of metallurgical coke. *Steel Res. Int.* **2017**, *88*, 1700063. [[CrossRef](#)]
64. Xu, R.S.; Dai, B.W.; Wang, W.; Johannes, S.; Bhattagaryya, A.; Xue, Z.L. Gasification reactivity and structure evolution of metallurgical coke under H₂O/CO₂ atmosphere. *Energy Fuels* **2018**, *32*, 1188–1195. [[CrossRef](#)]
65. Sun, Y.; Dou, M.H.; Wang, J.J.; Guo, R.; Sun, Z.; Liang, Y.H. Solution loss characteristics of cokes in coke-sinter coupling reaction. *China Metall.* **2021**, *31*, 15–19.
66. Lan, C.C.; Liu, R.; Zhang, S.H.; Lyu, Q. Effect of H₂ volume percent on gasification reaction of coke in blast furnace. *Iron Steel* **2020**, *55*, 100–106.
67. Lan, C.C.; Zhang, S.H.; Liu, X.J.; Liu, R.; Lyu, Q. Gasification behaviors of coke in a blast furnace with and without H₂. *ISIJ Int.* **2021**, *61*, 158–166. [[CrossRef](#)]
68. Qie, Y.N. *Study on Smelting Process of Blast Furnace with Gas-Injection*; North China University of Science and Technology: Tangshan, China, 2018.
69. Liu, C.Q. *Study on the New Technology of Coal-Injection into Blast Furnace-Study on the Reaction Thermodynamics and Kinetics of Blast Furnace with Coal Injection for Gasification*; North China University of Science and Technology: Tangshan, China, 2015.
70. Yan, C.J. *Experimental Study on Reduction of Iron Ore with Hydrogen-Rich Gas*; North China University of Science and Technology: Tangshan, China, 2017.
71. Li, F.M.; Lyu, Q.; Li, X.B. Influence of gas-injection from tuyeres on slag formation in blast furnace. *Iron Steel* **2007**, *42*, 12–15.
72. Lan, C.C.; Zhang, S.H.; Liu, X.J.; Lyu, Q.; Jiang, M.F. Change and mechanism analysis of the softening-melting behavior of the iron-bearing burden in a hydrogen-rich blast furnace. *Int. J. Hydrogen Energy* **2020**, *45*, 14255–14265. [[CrossRef](#)]
73. Li, J.P.; Lyu, Q.; Liu, S.; Liu, X.J. Effect of H₂ content on melt-dropping properties of burden. In Proceedings of the AISTech 2017, Nashville, TN, USA, 8–11 May 2017; Volume 1, pp. 569–575.
74. Yan, C.J.; Li, F.M.; Qie, Y.N.; Liu, S.; Lyu, Q. Effect of hydrogen content of bosh gas on iron ore dropping process. *J. Iron Steel Res.* **2017**, *29*, 441–446.
75. Du, C.B.; Liu, Z.J.; Zhang, J.L.; Wang, Y.Z.; Niu, L.L.; Kang, Q.F. Effect of hydrogen content on reduction and softening-melting properties of iron bearing charges. *China Metall.* **2018**, *28*, 19–23.
76. Yang, G.Q.; Zhang, J.L.; Chen, Y.X.; Wu, Q.Y.; Zhao, Z.Y.; Zhao, J. Influence of Hydrogen content of bosh gas on softening-melting property of iron-bearing burden material. *Iron Steel* **2012**, *47*, 14–18. [[CrossRef](#)]
77. Higuchi, K.; Matsuzaki, S.; Saito, K.; Nomura, S. Improvement in reduction behavior of sintered ores in a blast furnace through injection of reformed coke oven gas. *ISIJ Int.* **2020**, *60*, 2218–2227. [[CrossRef](#)]

78. Zhu, G.H. A review on hydrogen-enriched reduction in blast furnace. *Iron Steel* **2020**, *55*, 1–14.
79. Zhao, Z.G.; Yu, X.B.; Shen, Y.S.; Li, Y.T.; Xu, H.; Hu, Z.J. Model study of shaft injection of reformed coke oven gas in a blast furnace. *Energy Fuels* **2021**, *34*, 15048–15060. [[CrossRef](#)]
80. Heikkilä, A.M.; Koskela, A.M.; Iljana, M.O.; Lin, R.; Bartusch, H.; Heikkinen, E.P.; Fabritius, T.M. Coke gasification in blast furnace shaft conditions with H₂ and H₂O containing atmospheres. *Steel Res. Int.* **2021**, *92*, 2000456. [[CrossRef](#)]
81. Barrett, N.; Mitra, S.; Doostmohammadi, H.; Odea, D.; Zulli, P.; Chew, S.; Honeyands, T. Assessment of blast furnace operational constraints in the presence of hydrogen injection. *ISIJ Int.* **2022**, *62*, 1168–1177. [[CrossRef](#)]
82. Nogami, H.; Kashiwaya, Y.; Yamada, D. Simulation of blast furnace operation with intensive hydrogen injection. *ISIJ Int.* **2012**, *52*, 1523–1527. [[CrossRef](#)]